Rotational diffusion in concentrated colloidal dispersions of hard spheres

Vittorio Degiorgio and Roberto Piazza
Dipartimento di Elettronica, Università di Pavia, 27100 Pavia, Italy

Robert B. Jones
Department of Physics, Queen Mary and Westfield College, Mile End Road, London E1 4NS, United Kingdom
(Received 13 March 1995)

We have performed depolarized dynamic light scattering measurements on suspensions of colloidal spherical particles made of a fluorinated polymer. Electrostatic interactions are screened by adding salt, so that the particles behave as hard spheres. By suspending the particles in an index-matching solvent (18% urea in water) we have been able to investigate a wide range of particle volume fractions Φ from the dilute suspension up to 55%. The partially crystalline internal structure of fluorinated polymer colloids gives rise to a significant depolarized component in the scattered light field. By studying the temporal fluctuations of the depolarized component we can evaluate the short-time self-translational and rotational diffusion coefficients of the particles over the whole colloidal fluid phase and within the hard-sphere colloidal crystal. We also analyze the full shape of the rotational correlation function, which deviates from an exponential behavior in concentrated suspensions. Starting from the generalized Smoluchowski equation, we calculate the Φ dependence of the rotational diffusion coefficient up to the Φ^2 term and we discuss the validity of the approximation that decouples translational from rotational motion. We find good agreement between theoretical and experimental results.

PACS number(s): 82.70.Dd, 05.40.+j

I. INTRODUCTION

In recent years dynamic light scattering has been widely used for the investigation of the Brownian motion of interacting colloidal particles [1,2]. Both the collective and single-particle translational diffusion coefficients of hard spherical colloids have been measured as functions of the particle volume fraction Φ. The results have been compared with calculations based on the generalized Smoluchowski equation including hydrodynamic interactions. Some years ago, the theory was extended to include rotational diffusion [3]. It is well known that rotational diffusion can be investigated by dynamic depolarized light scattering (DDLS) from dispersions of anisotropic particles. However, if one has to rely on form anisotropy, the experiment becomes feasible only with large particles possessing a strongly nonspherical shape, whereas theoretical studies to date have dealt only with spherical particles. By using DDLS from spherical colloids that present an intrinsic optical anisotropy due to a partially crystalline internal structure [4,5], the first measurement of the concentration dependence of the rotational diffusion coefficient of spherical Brownian particles was recently performed [6]. The Φ dependence of the diffusion coefficients can be conveniently expressed by a series expansion in powers of Φ. In the case of the translational self-diffusion coefficient the available theoretical and experimental results go beyond the linear approximation, whereas in the case of rotational diffusion only the linear term is known.

In this article we present experimental and theoretical results concerning orientational relaxation in hard-sphere colloidal suspensions. By using index-matched suspensions, it is possible to perform measurements in a wide range of volume fractions extending to the colloidal-crystal region. The data give the full shape of the orientational correlation function $F_r(t)$, which shows an increasing deviation from exponential behavior as Φ grows. For $\Phi < 0.2$ such a deviation shows an interesting scaling property, in agreement with the theoretical predictions. From $F_r(t)$ we derive the Φ-dependent short-time rotational diffusion coefficient. The theoretical results include the calculation of the coefficient of the Φ^2 term in the series expansion of the short-time rotational diffusion coefficient. The calculation takes into account lowest-order three-body hydrodynamic effects. We have good agreement between theoretical and experimental results. In particular, it is found that the coefficient of the Φ^2 term has the same (negative) sign as does the linear term. Such behavior is different from that found for translational self-diffusion. In addition to the orientational correlation function, our experiment also gives the self-translational correlation function $F_s(t)$. It should be noted that $F_s(t)$ is measured with much better accuracy than in previous measurements and without using any specific tagging of particles.

The organization of the paper is as follows. In Sec. II we recall the main formulas of the DDLS theory. In Secs. III and IV we present the theoretical results concerning the Φ dependence of the rotational diffusion coefficient and in Sec. V we discuss the validity of the decoupling approximation that is used in the interpretation of the dynamic light scattering results. In Sec. VI we describe the experiment and we report the experimental data. In Sec. VII we compare our data with theory.

II. LIGHT SCATTERING FROM ANISOTROPIC PARTICLES

We consider spherical particles of radius a, made of an anisotropic material characterized by a polarizability tensor $\boldsymbol{\alpha}$. We assume cylindrical symmetry for $\boldsymbol{\alpha}$ along a main optical axis and call α_1, α_1, and α_3 the diagonal components of the polarizability tensor in the particle-fixed frame. The average polarizability of the particle is $\alpha_p = (\alpha_3 + 2\alpha_1)/3$ and the average index of refraction of the material constituting the particle is $n_p = (1+\alpha_p/V_p)^{1/2}$, where $V_p = 4\pi(a^3/3)$ is the particle volume. We call β the anisotropy of the particle polarizability $\beta = \alpha_3 - \alpha_1$. It is assumed that the light scattering treatment can be made under the Rayleigh-Debye (also called Rayleigh-Gans) approximation. For particles made of isotropic material the condition of validity of the Rayleigh-Debye approximation is $(4\pi/\lambda)a(n_p - n_s) \ll 1$, where λ is the wavelength of light and n_s is the index of refraction of the suspending medium. In the case of anisotropic particles, there is an additional condition for the validity of the approximation: $(4\pi/\lambda)a(n_3 - n_1) \ll 1$, where $n_3 = (1+\alpha_3/V_p)^{1/2}$ and $n_1 = (1+\alpha_1/V_p)^{1/2}$.

We consider the situation in which the incident field is linearly polarized in the vertical direction and the scattered field is observed in the horizontal plane. Because of the particle anisotropy the total scattered field is the superposition of two terms: the first is a vertically polarized component with amplitude proportional to the optical mismatch between particle and solvent; the second is a depolarized component with amplitude proportional to the internal particle anisotropy β. The temporal fluctuations of the first term are due to the translational motion of the particles, whereas the dynamics of the second term contains information about both translational and rotational motion. The second term gives rise to the horizontally polarized scattered field E_{VH}.

The correlation function of E_{VH} is defined as

$$G_{VH}(t) = \langle E_{VH}(0)E^*_{VH}(t)\rangle \quad . \tag{1}$$

The dynamic light scattering experiment gives the modulus of the correlation function, which can be written as

$$|G_{VH}(t)| = AI_0 \sum_{j,k}^{N} \langle \alpha_{VHj}(0)\alpha_{VHk}(t) \times \exp\{i\boldsymbol{k}\cdot[\boldsymbol{R}_j(0) - \boldsymbol{R}_k(t)]\}\rangle \quad , \tag{2}$$

where A is a constant, I_0 is the incident intensity, N is the number of particles within the scattering volume, $\boldsymbol{R}_j(t)$ is the position of the jth particle at time t, and $\boldsymbol{k}$ is the scattering vector with modulus $k = (4\pi n_s/\lambda)\sin(\theta/2)$, θ being the scattering angle. The quantity α_{VHj} is given by

$$\alpha_{VHj} = i\sqrt{2\pi/15}\,\beta\,[Y_{2,1}(\Omega_j(t)) + Y_{2,-1}(\Omega_j(t))] \quad , \tag{3}$$

where $Y_{2,\pm1}$ are the second-order spherical harmonic functions of index ±1 and $\Omega(t)$ denotes the polar angles $\delta(t)$,$\phi(t)$, which specify the direction of the main optical axis of the tracer particle at time t. Assuming that the orientations of the optical axis of different particles are uncorrelated and observing that $\langle Y_{2,\pm1}(\Omega_j(t))\rangle = 0$, all the cross terms in the expression for G_{VH} disappear. If the N particles are identical, we have

$$|G_{VH}(t)| = AI_0N\langle \alpha_{VHj}(0)\alpha_{VHj}(t) \times \exp\{i\boldsymbol{k}\cdot[\boldsymbol{R}_j(0) - \boldsymbol{R}_j(t)]\}\rangle \quad . \tag{4}$$

Here j denotes any one of the N particles that can be regarded as a tracer particle. Note that, for scattering angle tending to 0, that is, $\boldsymbol{k} \to \boldsymbol{0}$, $|G_{VH}(t)|$ becomes proportional to the rotational single particle (tracer) correlation function $F_r(t)$ defined as [7]

$$F_r(t) = 4\pi\ \langle Y^*_{2,1}(\Omega_j(0))Y_{2,1}(\Omega_j(t))\rangle \quad . \tag{5}$$

If we assume that the orientation of the particle is decoupled from the particle's translation, the expression for $|G_{VH}(t)|$ becomes

$$|G_{VH}(t)| = AI_0NF_r(t)F_s(k,t), \tag{6}$$

where

$$F_s(k,t) = \langle \exp\{i\boldsymbol{k}\cdot[\boldsymbol{R}_j(0) - \boldsymbol{R}_j(t)]\}\rangle \tag{7}$$

is the translational self-correlation function (self-dynamic structure factor). In the case of hard spheres, the decoupling hypothesis is rigorously true at short times as we discuss below and is expected to be approximately satisfied at all times.

In the case of spherical noninteracting particles, the functions F_s and F_r are exponential:

$$F_s(k,t) = \exp(-k^2D_0^t t), \quad F_r(t) = \exp(-6D_0^r t), \tag{8}$$

where D_0^t and D_0^r are, respectively, the translational and rotational diffusion coefficients of a single particle at infinite dilution. We recall that $D_0^t = k_BT/(6\pi\eta a)$ and $D_0^r = k_BT/(8\pi\eta a^3)$, where η is the shear viscosity of the suspending fluid. The first cumulant of G_{VH} , for noninteracting particles, is given by

$$\Gamma_{VH0} = D_0^t k^2 + 6D_0^r. \tag{9}$$

III. ROTATIONAL DIFFUSION COEFFICIENT

Under the assumptions made in the preceding section that orientations of different particles are uncorrelated (no orientation-dependent interactions) and that translational and orientational correlations are uncoupled, we can use DDLS to measure the correlation function $F_r(t)$. This correlation function is a special case of the set of correlation functions studied in Ref. [3] and defined by Berne and Pecora [7] as

$$C_{\ell'm';\ell m}(t) = \langle Y^*_{\ell'm'}(\Omega_1(0))Y_{\ell m}(\Omega_1(t))\rangle \quad . \tag{10}$$

For a rotationally invariant system these correlation functions are real and diagonal in ℓ and m [8],

$$C_{\ell' m';\ell m}(t) = \frac{\delta_{\ell'\ell}\delta_{m'm}}{4\pi} C_\ell(t) \quad ,$$
$$C_\ell(t) = \langle P_\ell\left(\boldsymbol{n}_1(0)\cdot\boldsymbol{n}_1(t)\right)\rangle \quad . \tag{11}$$

Here P_ℓ is a Legendre polynomial and $\boldsymbol{n}_1(t)$ is a unit vector that is parallel to the optical axis of particle 1 at time t. Thus the experimentally measured $F_r(t)$ can be expressed as

$$F_r(t) = C_2(t). \tag{12}$$

The short-time rotational self-diffusion coefficient D_r^S is defined in the following way by the short-time behavior of these correlation functions:

$$\ell(\ell+1)D_r^S = -\left.\frac{d\ln C_\ell(t)}{dt}\right|_{t\to 0} \quad . \tag{13}$$

For noninteracting hard spheres of radius a the diffusion coefficient D_r^S is the same as D_0^r, which was defined in Sec. II. In such a non-interacting suspension the correlation function $C_\ell(t)$ is an exponential for all times and all ℓ values,

$$C_\ell(t) = C_\ell^0(t) = \exp[-\ell(\ell+1)D_0^r t] \quad . \tag{14}$$

The existence of direct interparticle interactions (here assumed to occur through spherically symmetric pair potentials) and of hydrodynamic interactions (many body in nature) means that the short-time rotational diffusion coefficient D_r^S becomes a function of the volume fraction Φ of suspended particles. In addition, the measured correlation function ceases to be exponential so that we can write $C_\ell(t) \approx \exp[-\ell(\ell+1)D_r^S t]$ only in the limit $t \to 0$.

The short-time coefficient D_r^S measures the initial mean-square displacement of the unit vector $\boldsymbol{n}(t)$ on the surface of a unit sphere. At longer times, because the unit sphere is a bounded and periodic surface, we cannot make such an interpretation of rotational diffusion.

For interacting systems the long-time behavior of $C_\ell(t)$ is best interpreted in Fourier representation in terms of a frequency-dependent relaxation time $\tau_\ell(\omega)$ defined by

$$\hat{C}_\ell(\omega) = \int_0^\infty e^{i\omega t} C_\ell(t)dt = \frac{1}{-i\omega + \tau_\ell^{-1}(\omega)} \quad . \tag{15}$$

The short-time rotational diffusion constant is related to the relaxation time at infinite frequency $\ell(\ell+1)D_r^S = \tau_\ell^{-1}(\infty)$, while the zero-frequency limit of $\tau_\ell(\omega)$ defines a mean correlation time studied in Ref. [8],

$$\tau_\ell(0) = \int_0^\infty C_\ell(t)dt \quad . \tag{16}$$

To model these experimentally measurable quantities we must specify the dynamics of the suspension. On the time scale of dynamic light scattering observations (times longer than the momentum relaxation times of the colloidal particles) the generalized Smoluchowski equation (GSE) provides a good description of the dynamics of the suspension [1,2]. The time correlation functions can be expressed in terms of the adjoint Smoluchowski operator $\mathcal{L}$ and the equilibrium solution to the GSE, $P_e(X)$. Here we use X to denote the configuration of the suspension in both position and orientation, $X = (\boldsymbol{R}_1, \ldots, \boldsymbol{R}_N, \boldsymbol{n}_1, \ldots, \boldsymbol{n}_N)$, where $\boldsymbol{R}_i$ is the position of the center of particle i and $\boldsymbol{n}_i$ is its orientation vector. As an abbreviation we will also write $X = (X_t, X_r)$ with $X_t = (\boldsymbol{R}_1, \ldots, \boldsymbol{R}_N)$ and $X_r = (\boldsymbol{n}_1, \ldots, \boldsymbol{n}_N)$. The equilibrium distribution function for the suspension as a whole $P_e(X)$ is given by

$$P_e(X) = \frac{1}{Z}\exp[-V(X)/k_BT] \quad , \tag{17}$$

where Z is a normalization factor and $V(X)$ is the potential-energy function for the suspension. We assume that V consists of a sum of spherically symmetric two-body potentials that do not depend on particle orientation so that $V(X) = V(X_t)$. With this assumption the adjoint Smoluchowski operator takes the form

$$\mathcal{L} = \sum_{i,j=1}^{N}\left\{\left[\frac{\partial}{\partial \boldsymbol{R}_i} - \frac{1}{k_BT}\left(\frac{\partial V}{\partial \boldsymbol{R}_i}\right)\right]\cdot\left[\boldsymbol{D}_{ij}^{tt}\cdot\frac{\partial}{\partial \boldsymbol{R}_j} + \boldsymbol{D}_{ij}^{tr}\cdot\boldsymbol{L}_j\right] + \boldsymbol{L}_i\cdot\left[\boldsymbol{D}_{ij}^{rt}\cdot\frac{\partial}{\partial \boldsymbol{R}_j} + \boldsymbol{D}_{ij}^{rr}\cdot\boldsymbol{L}_j\right]\right\}. \tag{18}$$

Here $\boldsymbol{L}_i = \boldsymbol{n}_i \times \partial/\partial\boldsymbol{n}_i$ is the gradient in orientation space [3] and the diffusion tensors $\boldsymbol{D}_{ij}^{ab}$ are defined in terms of elements of the grand mobility matrix [9–11] for the suspension $\boldsymbol{\mu}_{ij}^{ab}$,

$$\boldsymbol{D}_{ij}^{ab} = k_BT\boldsymbol{\mu}_{ij}^{ab}(X_t) \quad . \tag{19}$$

The mobility tensors embody the hydrodynamic interactions between the colloidal particles, which are many body in character and not representable as a sum of pair interactions except at low densities. Note that the mobility tensors depend on the positions of the particles but not on their orientations. This is true only for spherical particles; for nonspherical particles the hydrodynamic forces couple position and orientation variables. In terms of the time translation operator $\mathcal{L}$ the correlation function $C_{\ell' m';\ell m}(t)$ can be written as

$$C_{\ell' m';\ell m}(t) = \frac{1}{Z}\int dX e^{-V(X_t)/k_BT} \times Y_{\ell' m'}^*(\Omega_1)\, e^{\mathcal{L}t} Y_{\ell m}(\Omega_1). \tag{20}$$

As shown elsewhere [1,3], we can express the short-time rotational self-diffusion coefficient in the form

$$D_r^S = D_0^r H_s^r \quad ,$$
$$H_s^r = \frac{1}{3D_0^r}\langle \mathrm{Tr}\boldsymbol{D}_{11}^{rr}\rangle = \frac{k_BT}{3D_0^r}\langle \mathrm{Tr}\boldsymbol{\mu}_{11}^{rr}\rangle$$
$$= \frac{k_BT}{3D_0^r}\int dX P_e(X_t)\mathrm{Tr}\boldsymbol{\mu}_{11}^{rr}(X_t) \quad . \tag{21}$$

The function H_s^r, which is volume fraction dependent, is given as an equilibrium average over the trace of the rotation-rotation part of the tracer particle mobility tensor. Because of the X_t dependence in the distribution function P_e and in the mobility tensor, the value of H_s^r depends on both direct and hydrodynamic interactions.

IV. VIRIAL EXPANSION

The equilibrium average of the rotational mobility tensor is difficult to calculate, even for hard-sphere pair interactions, because of the many-body character of the hydrodynamic interactions. For moderate volume fractions Φ of colloidal particles it is useful to evaluate H_s^r as a virial series

$$H_s^r = 1 + H_{s1}^r \Phi + H_{s2}^r \Phi^2 + \cdots \quad . \tag{22}$$

We recall that for the short-time translational self-diffusion coefficient an exactly similar result holds [1],

$$\begin{aligned} D_t^S &= D_0^t H_s^t, \quad D_0^t = k_B T/6\pi\eta a, \\ H_s^t &= \frac{1}{3D_0^t}\langle \mathrm{Tr} \boldsymbol{D}_{11}^{tt}\rangle = \frac{k_B T}{3D_0^t}\langle \mathrm{Tr}\boldsymbol{\mu}_{11}^{tt}\rangle \quad , \\ H_s^t &= 1 + H_{s1}^t \Phi + H_{s2}^t \Phi^2 + \cdots \quad . \end{aligned} \tag{23}$$

The coefficients of the linear terms H_{s1}^t, H_{s1}^r can be calculated accurately from the two-body direct and hydrodynamic interactions [3,12,13] as

$$H_{s1}^t = -1.831, \quad H_{s1}^r = -0.630 \quad . \tag{24}$$

The importance of many-body hydrodynamic interactions was first demonstrated by Beenakker and Mazur [14], who calculated the lowest-order three-body contribution to H_{s2}^t. This term was of order R^{-7}, where R is a typical interparticle spacing. To order Φ^2 they reported

$$H_{s2}^t = -0.93 + 1.80 = 0.88 \quad , \tag{25}$$

where the term -0.93 arises from two-particle hydrodynamic interactions averaged over the order Φ^2 part of the pair distribution function while the term 1.80 is the lowest-order three-particle hydrodynamic interaction contribution. Here the many-body hydrodynamic interactions are so important that they change the sign of the second virial coefficient.

It is of interest to see whether a similar sign reversal occurs in the second virial coefficient for the rotational self-diffusion coefficient. The virial expansion of the many-body average in (21) is best carried out by use of a rooted cluster expansion [3,15]. The result of such an expansion is expressible as

$$\begin{aligned} \langle \boldsymbol{\mu}_{11}^{rr}\rangle = \boldsymbol{\mu}_{11}^{rr}(\boldsymbol{R}_1) &+ \frac{n_0^2}{N}\int d\boldsymbol{R}_1 d\boldsymbol{R}_2\, g(\boldsymbol{R}_1,\boldsymbol{R}_2)\,[\boldsymbol{\mu}_{11}^{rr}(\boldsymbol{R}_1,\boldsymbol{R}_2) - \boldsymbol{\mu}_{11}^{rr}(\boldsymbol{R}_1)] \\ &+ \frac{n_0^3}{2N}\int d\boldsymbol{R}_1 d\boldsymbol{R}_2 d\boldsymbol{R}_3\, g(\boldsymbol{R}_1,\boldsymbol{R}_2,\boldsymbol{R}_3)\{[\boldsymbol{\mu}_{11}^{rr}(\boldsymbol{R}_1,\boldsymbol{R}_2,\boldsymbol{R}_3) - \boldsymbol{\mu}_{11}^{rr}(\boldsymbol{R}_1)] \\ &- [\boldsymbol{\mu}_{11}^{rr}(\boldsymbol{R}_1,\boldsymbol{R}_2) - \boldsymbol{\mu}_{11}^{rr}(\boldsymbol{R}_1)] - [\boldsymbol{\mu}_{11}^{rr}(\boldsymbol{R}_1,\boldsymbol{R}_3) - \boldsymbol{\mu}_{11}^{rr}(\boldsymbol{R}_1)]\} + \cdots, \end{aligned} \tag{26}$$

where $g(\boldsymbol{R}_1,\boldsymbol{R}_2)$ and $g(\boldsymbol{R}_1,\boldsymbol{R}_2,\boldsymbol{R}_3)$ are the pair and triplet distribution functions for the suspension, n_0 is the number density, and N is the total number of suspended particles. In the thermodynamic limit the suspension is translation invariant so that the distribution functions and mobilities depend only on the relative positions of the particles $\boldsymbol{R}_{ij} = \boldsymbol{R}_j - \boldsymbol{R}_i$. Note that the combinations of mobilities that occur in the cluster expansion ensure that all long distance divergences are eliminated from the integrations. In the three-body term this ensures also that contributions to the three-body interactions that are superpositions of pair interactions are also subtracted out, leaving only irreducible three-body mobility contributions.

The structure of the two-body mobility tensor $\boldsymbol{\mu}_{11}^{rr}$ has been given by Schmitz and Felderhof [9] in terms of two independent scalar functions of relative separation $\alpha_{11}^{rr}(R_{12})$ and $\beta_{11}^{rr}(R_{12})$. Using translation invariance we can reduce the two-body contribution to the cluster expansion to the form

$$\begin{aligned} \langle \boldsymbol{\mu}_{11}^{rr}\rangle_{\text{two-body}} = D_0^r \mathbf{1}\Bigg(1 &+ \frac{\Phi}{a^3}\int_{2a}^{\infty} R^2 dR g(R) \\ &\times\{8\pi\eta a^3[\alpha_{11}^{rr}(R) - \beta_{11}^{rr}(R)] \\ &+3[8\pi\eta a^3\beta_{11}^{rr}(R) - 1]\}\Bigg), \end{aligned} \tag{27}$$

where $\mathbf{1}$ is the unit tensor, $\Phi = (4/3)\pi a^3 n_0$ is the volume fraction of suspended spheres, $R = R_{12}$, and $g(R)$ is the pair distribution function for a hard-sphere gas. The functions α_{11}^{rr} and β_{11}^{rr} can be calculated as series expansions in powers of $2a/R$ to arbitrary order [10]. The hard-sphere pair distribution function has its own virial expansion as [16]

$$g(R) = g_0(R) + \Phi g_1(R) + \cdots, \tag{28}$$

where

$$g_0(R) = \begin{cases} 0, & R < 2a \\ 1, & R \geq 2a \end{cases} \tag{29}$$

and

$$g_1(R) = \begin{cases} 8 - 3\frac{R}{a} + \frac{1}{16}\left(\frac{R}{a}\right)^3, & 2a \leq R \leq 4a \\ 0 \quad \text{otherwise.} \end{cases} \tag{30}$$

The integrals in (27) can be calculated to any desired accuracy by use of the series expansions for α_{11}^{rr} and β_{11}^{rr} together with a simple extrapolation procedure [13]. The result for the two-body contributions to H_s^r to three significant figures is

$$H_{s,\text{two-body}}^r = 1 - 0.630\Phi - 1.01\Phi^2 \quad . \tag{31}$$

For the translational self-diffusion coefficient [14] the contribution of two-body hydrodynamic interactions is given within an accuracy of a few percent by keeping only the terms in the series expansions through order R^{-6}. For the rotational case one needs to go to much higher order to get comparable accuracy. We note for later reference that if we kept series expansion terms only through order R^{-10}, then instead of the result in Eq. (31) we would get

$$H^r_{s,\text{two-body}} = 1 - 0.500\Phi - 0.723\Phi^2 \quad (\text{order } R^{-10}) \quad . \tag{32}$$

Turning now to the three-body hydrodynamic interaction effects we need keep only the lowest-order (in Φ) contribution to the triplet distribution function

$$g_0(\boldsymbol{R}_1, \boldsymbol{R}_2, \boldsymbol{R}_3) = \begin{cases} 1, & R_{12} \geq 2a,\ R_{13} \geq 2a,\ R_{23} \geq 2a \\ 0 & \text{otherwise} \end{cases} \quad . \tag{33}$$

Mazur and van Saarloos [17] have published explicit expressions for some of the low-order three-body contributions to the mobilities $\boldsymbol{\mu}^{tt}_{11}$ and $\boldsymbol{\mu}^{rr}_{11}$. However, the explicit contribution to the rotational mobility given by them (of order R^{-6} with R a typical interparticle separation) is in fact a superposition of two-body terms and hence is subtracted out of the order Φ^2 part of the cluster expansion. Instead, we require the lowest-order irreducible three-body contribution to $\boldsymbol{\mu}^{rr}_{11}(\boldsymbol{R}_1, \boldsymbol{R}_2, \boldsymbol{R}_3)$. This term is straightforward to calculate using the method of reflections given by Reuland, Felderhof, and Jones [18]. For the three-body mobility function for particle i, $\boldsymbol{\mu}^{rr}_{ii}$, we find the result

$$\begin{aligned} 8\pi\eta a^3 \boldsymbol{\mu}^{rr}_{ii,\text{three-sphere}} = \frac{75}{4} \sum_{k\neq i} \sum_{\ell \neq i,k} \left(\frac{a}{R_{ik}}\right)^3 \left(\frac{a}{R_{k\ell}}\right)^3 \left(\frac{a}{R_{i\ell}}\right)^3 \Bigg[\Bigg(& 5\xi_k\xi_\ell \sqrt{1-\xi_k^2}\sqrt{1-\xi_\ell^2} \\ & + \xi_i \sqrt{1-\xi_k^2}\sqrt{1-\xi_\ell^2} - \xi_k \sqrt{1-\xi_\ell^2}\sqrt{1-\xi_i^2} - \xi_\ell \sqrt{1-\xi_k^2}\sqrt{1-\xi_i^2} \Bigg) \hat{\boldsymbol{n}}_{ik\ell}\hat{\boldsymbol{n}}_{ik\ell} \\ & - \xi_k\xi_\ell(\xi_i \mathbf{1} - \hat{\boldsymbol{R}}_{ik}\hat{\boldsymbol{R}}_{i\ell}) \Bigg] + O((a/R)^{11}) \quad . \end{aligned} \tag{34}$$

In this equation $\hat{\boldsymbol{R}}_{pq} = \boldsymbol{R}_{pq}/|\boldsymbol{R}_{pq}|$, while $\xi_i = \hat{\boldsymbol{R}}_{ik} \cdot \hat{\boldsymbol{R}}_{i\ell}$, $\xi_k = \hat{\boldsymbol{R}}_{ki} \cdot \hat{\boldsymbol{R}}_{k\ell}$, and $\xi_\ell = \hat{\boldsymbol{R}}_{\ell i} \cdot \hat{\boldsymbol{R}}_{\ell k}$. The unit vector $\hat{\boldsymbol{n}}_{ik\ell}$ is normal to the triangle with vertices $\boldsymbol{R}_i$, $\boldsymbol{R}_k$, and $\boldsymbol{R}_\ell$.

With the above result we find that the trace of $\boldsymbol{\mu}^{rr}_{11}(\boldsymbol{R}_1, \boldsymbol{R}_2, \boldsymbol{R}_3)$ depends only on the internal variables of the triangle with vertices $\boldsymbol{R}_1$,$\boldsymbol{R}_2$, and $\boldsymbol{R}_3$, but not on the orientation or position of the triangle. This enables one to simplify the three-body integral in the cluster expansion (26) to the form

$$\begin{aligned} \frac{1}{3D_0^r} \langle \text{Tr} \boldsymbol{D}^{rr}_{11} \rangle_{\text{three-body}} & \\ = \Phi^2 \frac{225}{64} \int_0^1 dt_{12} \int_0^1 dt_{13} \int_{-1}^1 d\xi_1 g_0(t_{12}, t_{13}, \xi_1) & \\ \times f(t_{12}, t_{13}, \xi_1) \ , & \end{aligned} \tag{35}$$

where $t_{12} = 2a/R_{12}$, $t_{13} = 2a/R_{13}$, $\xi_1 = \hat{\boldsymbol{R}}_{12} \cdot \hat{\boldsymbol{R}}_{13}$, g_0 is the triplet distribution function, and the function $f(t_{12}, t_{13}, \xi_1)$ is defined by

$$\begin{aligned} f(t_{12}, t_{13}, \xi_1) = \frac{t_{12}^2 t_{13}^2}{h^{3/2}} \{ & 2\xi_1^2 - 1 - (t_{12} - t_{13}\xi_1) \\ & \times (t_{13} - t_{12}\xi_1)[(t_{12}^2 + t_{13}^2)\xi_1 \\ & - t_{12}t_{13}(5 - 3\xi_1^2)]/h^2 \} \ , \end{aligned} \tag{36}$$

with

$$h = h(t_{12}, t_{13}, \xi_1) = t_{12}^2 + t_{13}^2 - 2t_{12}t_{13}\xi_1 \quad . \tag{37}$$

Since the triplet distribution function $g_0(t_{12}, t_{13}, \xi_1)$ vanishes for overlap configurations of the three spheres, the domain of integration in (35) is complicated. However, we have used a Monte Carlo method to evaluate the integral and we find the result

$$\frac{1}{3D_0^r} \langle \text{Tr} \boldsymbol{D}^{rr}_{11} \rangle_{\text{three-body}} = 0.339\Phi^2 \quad . \tag{38}$$

If we combine the three-body result with the two-body contributions [correct to $O((a/R)^{10})$] given in (32), we find virial expansion coefficients

$$H^r_s = 1 - 0.500\Phi - 0.384\Phi^2 \quad (\text{order } R^{-10}) \quad , \tag{39}$$

while if we use the exact two-body contributions (31) we get

$$H^r_s = 1 - 0.630\Phi - 0.67\Phi^2 \quad . \tag{40}$$

Although, just as in the case of the translational self-diffusion coefficient [14], higher-order three-body interactions will slightly change the magnitude of the coefficient of Φ^2 given by the lowest-order term in Eq. (38), it is clear that the second virial coefficient of H^r_s remains negative unlike that for H^t_s, whose sign is changed by many-body effects.

V. THE DECOUPLING APPROXIMATION

As shown in Sec. II, dynamic light scattering from optically anisotropic particles measures correlation functions of the form

$$F^{\ell}_{m'm}(\boldsymbol{k},t) = \frac{4\pi}{N}\sum_{i,j=1}^{N}\langle Y^{*}_{\ell m'}(\Omega_i(0))Y_{\ell m}(\Omega_j(t)) \times e^{i\boldsymbol{k}\cdot[\boldsymbol{R}_i(0)-\boldsymbol{R}_j(t)]}\rangle \quad . \tag{41}$$

If we assume, as in Sec. II, that (i) orientational motions of different particles are uncorrelated and (ii) translational and orientational motions of a single particle are uncorrelated, then the correlation function above simplifies to give the result

$$\begin{aligned} F^{\ell}_{m'm}(\boldsymbol{k},t) &= 4\pi\langle Y^{*}_{\ell m'}(\Omega_1(0))Y_{\ell m}(\Omega_1(t))\rangle \times\langle e^{i\boldsymbol{k}\cdot[\boldsymbol{R}_1(0)-\boldsymbol{R}_1(t)]}\rangle \\ &= 4\pi C_{\ell m';\ell m}(t)F_s(\boldsymbol{k},t) \\ &= \delta_{m'm}C_{\ell}(t)F_s(\boldsymbol{k},t), \end{aligned} \tag{42}$$

which we may call the decoupling approximation. The assumptions above are valid for dilute suspensions of spherical particles with short-range direct forces where different particles are uncorrelated and where translation and rotation of a single particle are uncoupled for symmetry reasons. However, in more dense suspensions these assumptions are not obviously satisfied. For example, in the systems considered here the hydrodynamic interactions mean that the relaxation of the orientation $\boldsymbol{n}_j$ of particle j is coupled to the position $\boldsymbol{R}_i$ of particle i through the position dependence of $\boldsymbol{D}^{rr}_{jj}(X_t)$, so that the assumptions of the decoupling approximation are not met. Nevertheless, if the direct interactions described by $V(X)$ are orientation independent $[V(X) = V(X_t)]$ and if the GSE describes the dynamics of the system, the decoupling approximation is exact at short times.

To see this, we first write Eq. (41) as

$$F^{\ell}_{m'm}(\boldsymbol{k},t) = \frac{4\pi}{N}\sum_{i,j=1}^{N}\langle Y^{*}_{\ell m'}(\Omega_i)e^{i\boldsymbol{k}\cdot\boldsymbol{R}_i}e^{\mathcal{L}t}Y_{\ell m}(\Omega_j)e^{-i\boldsymbol{k}\cdot\boldsymbol{R}_j}\rangle, \tag{43}$$

where the thermal average takes the form

$$\langle(\cdots)\rangle = \frac{1}{Z_t(4\pi)^N}\int d\Omega_1\cdots d\Omega_N\int d\boldsymbol{R}_1\cdots d\boldsymbol{R}_N\ (\cdots),$$
$$Z_t = \int d\boldsymbol{R}_1\cdots d\boldsymbol{R}_N \exp[-V(X_t)/k_BT] \quad . \tag{44}$$

We observe from (18) that the operator $\mathcal{L}$ contains no term that can couple Ω_i to Ω_j . Therefore, in the thermal average, by orthonormality of spherical harmonics, all collective terms $(i \neq j)$ vanish so that $F^{\ell}_{m'm}(\boldsymbol{k},t)$ reduces to a sum of self-correlations, which, for identical particles, can be further reduced to the simple expression

$$F^{\ell}_{m'm}(\boldsymbol{k},t) = 4\pi\langle Y^{*}_{\ell m'}(\Omega_1)e^{i\boldsymbol{k}\cdot\boldsymbol{R}_1}e^{\mathcal{L}t}Y_{\ell m}(\Omega_1)e^{-i\boldsymbol{k}\cdot\boldsymbol{R}_1}\rangle \quad . \tag{45}$$

The operator $\mathcal{L}$ is given in (18) as a sum of four parts, which we write in an obvious notation as

$$\mathcal{L} = \mathcal{L}^{tt} + \mathcal{L}^{tr} + \mathcal{L}^{rt} + \mathcal{L}^{rr} \quad . \tag{46}$$

The four parts of the operator do not commute with each other because the translation operators $\partial/\partial\boldsymbol{R}_i$ do not commute with the position-dependent diffusion tensors $\boldsymbol{D}^{ab}_{ij}(X_t)$. This lack of commutativity tells us that the decoupling approximation cannot be exact. However, we can say something more at short times when we can write the correlation function to order t as

$$\begin{aligned} F^{\ell}_{m'm}(\boldsymbol{k},t) = {} & 4\pi\langle Y^{*}_{\ell m'}(\Omega_1)Y_{\ell m}(\Omega_1)\rangle \\ & + t\ 4\pi\langle Y^{*}_{\ell m'}(\Omega_1)e^{i\boldsymbol{k}\cdot\boldsymbol{R}_1}\mathcal{L}Y_{\ell m}(\Omega_1)e^{-i\boldsymbol{k}\cdot\boldsymbol{R}_1}\rangle \\ & + O(t^2) \quad . \end{aligned} \tag{47}$$

In the term of order t we insert the expression (46) so that we must consider

$$4\pi\langle Y^{*}_{\ell m'}(\Omega_1)e^{i\boldsymbol{k}\cdot\boldsymbol{R}_1}(\mathcal{L}^{tt}+\mathcal{L}^{tr}+\mathcal{L}^{rt}+\mathcal{L}^{rr}) \times Y_{\ell m}(\Omega_1)e^{-i\boldsymbol{k}\cdot\boldsymbol{R}_1}\rangle \quad . \tag{48}$$

It is now straightforward to use the orthonormality properties of the spherical harmonics together with appropriate symmetry properties to simplify the parts of Eq. (47). For the zeroth-order term we have trivially

$$4\pi\langle Y^{*}_{\ell m'}(\Omega_1)Y_{\ell m}(\Omega_1)\rangle = \delta_{m'm} \quad . \tag{49}$$

For the contribution of $\mathcal{L}^{tt}$ to the expression given in (48) we have, using isotropy,

$$\begin{aligned} & 4\pi\langle Y^{*}_{\ell m'}(\Omega_1)e^{i\boldsymbol{k}\cdot\boldsymbol{R}_1}\mathcal{L}^{tt}\,Y_{\ell m}(\Omega_1)e^{-i\boldsymbol{k}\cdot\boldsymbol{R}_1}\rangle \\ & \quad = 4\pi\langle Y^{*}_{\ell m'}(\Omega_1)Y_{\ell m}(\Omega_1)\rangle\langle e^{i\boldsymbol{k}\cdot\boldsymbol{R}_1}\mathcal{L}^{tt}\,e^{-i\boldsymbol{k}\cdot\boldsymbol{R}_1}\rangle \\ & \quad = -\delta_{m'm}\frac{k^2}{3}\langle \mathrm{Tr}\boldsymbol{D}^{tt}_{11}\rangle \quad . \end{aligned} \tag{50}$$

For a translation-rotation component such as $\mathcal{L}^{rt}$ we have

$$\begin{aligned} & 4\pi\langle Y^{*}_{\ell m'}(\Omega_1)e^{i\boldsymbol{k}\cdot\boldsymbol{R}_1}\mathcal{L}^{rt}\,Y_{\ell m}(\Omega_1)e^{-i\boldsymbol{K}\cdot\boldsymbol{R}_1}\rangle \\ & \quad = -4\pi\langle Y^{*}_{\ell m'}(\Omega_1)\boldsymbol{L}_1Y_{\ell m}(\Omega_1)\rangle\cdot\langle\boldsymbol{D}^{rt}_{11}\rangle\cdot i\boldsymbol{k} \quad . \end{aligned} \tag{51}$$

In an isotropic suspension, $\langle\boldsymbol{D}^{rt}_{11}\rangle$ vanishes by a parity argument so that there is no contribution from $\mathcal{L}^{rt}$. An exactly similar argument shows that $\mathcal{L}^{tr}$ makes no contribution either. Finally, for $\mathcal{L}^{rr}$, using isotropy again, we find

$$\begin{aligned} & 4\pi\langle Y^{*}_{\ell m'}(\Omega_1)e^{i\boldsymbol{k}\cdot\boldsymbol{R}_1}\mathcal{L}^{rr}\,Y_{\ell m}(\Omega_1)e^{-i\boldsymbol{k}\cdot\boldsymbol{R}_1}\rangle \\ & \quad = -\delta_{m'm}\frac{\ell(\ell+1)}{3}\langle\mathrm{Tr}\boldsymbol{D}^{rr}_{11}\rangle \quad . \end{aligned} \tag{52}$$

Putting these results together gives, to first order in t,

$$\begin{aligned} F^{\ell}_{m'm}(\boldsymbol{k},t) = \delta_{m'm}\{1 - & \left[k^2D^t_0H^t_s + \ell(\ell+1)D^r_0H^r_s\right]t \\ & + O(t^2)\} \quad , \end{aligned} \tag{53}$$

which is exactly the result of the decoupling approximation (42) to order t. Thus, for short-time measurements the decoupling is exact; translation-rotation coupling effects appear only at order t^2, where terms such as

$$\frac{t^2}{2}\, k_\beta \langle L_{1\alpha} Y^*_{\ell m'}(\Omega_1) L_{1\rho} Y_{\ell m}(\Omega_1)\rangle \langle D^{rt}_{11\alpha\beta} D^{rt}_{11\rho\sigma}\rangle\, k_\sigma \quad (54)$$

break the decoupling approximation.

Even within the decoupling approximation Eq. (42), the correlation function $C_\ell(t)$ contains rotation-translation coupling effects at long times because, in the time translation operator $\mathcal{L}$ that occurs in Eq. (20), the operators $\mathcal{L}^{tt}$, $\mathcal{L}^{tr}$, and $\mathcal{L}^{rt}$ do not commute with $\mathcal{L}^{rr}$. If we neglect these coupling effects it is possible, for a dilute suspension, to derive an explicit result for $C_\ell(t)$ at longer times, which can be compared with experimental measurements. The physical idea is to allow the particles to carry out rotational time evolution while holding their positions fixed, which corresponds to making the replacement $\mathcal{L} \to \mathcal{L}^{\rm rr}$ in the definition of $C_{\ell' m';\ell m}(t)$ given in Eq. (20). As discussed in detail elsewhere [8] it is then possible, working to first order in Φ, to obtain a closed form expression for $C_\ell(t)$ that incorporates two-body direct and hydrodynamic interactions.

In the absence of interactions between particles the correlation function $C_\ell(t)$ becomes a pure exponential $C^0_\ell(t)$ as given in Eq. (14). The interactions modify the shape of $C_\ell(t)$. We can express the deviations from pure exponential behavior by a virial expansion [8]

$$\frac{C_\ell(t)}{C^0_\ell(t)} = 1 + \Phi\gamma_\ell(t) + \cdots \quad , \quad (55)$$

where $\gamma_\ell(t)$ is given explicitly in Ref. [8] as

$$\gamma_\ell(t) = \frac{3}{(2\ell+1)a^3}\int_{2a}^{\infty} dR\, R^2 e^{-v(R)/k_BT} \times \sum_{q=-\ell}^{\ell}\left(\exp\left\{-k_BT\left[\ell(\ell+1)\left(\beta^{rr}_{11} - \frac{D^r_0}{k_BT}\right) + (\alpha^{rr}_{11} - \beta^{rr}_{11})q^2\right]t\right\} - 1\right). \quad (56)$$

Here $v(R)$ is the two-body pair potential representing direct interactions while $\alpha^{rr}_{11}(R)$ and $\beta^{rr}_{11}(R)$ are the same two-body mobility functions that occur above in Eq. (27). For a hard-sphere pair potential, $\gamma_2(t)$ has been computed numerically and reported in [8]. At short times the results given in Eqs. (55) and (56) reduce to give the order Φ result H^r_{s1}, quoted above in Eq. (24). At longer times the effect of the hydrodynamic interactions is to slow down the decay of $C_\ell(t)$ relative to the exponential decay of $C^0_\ell(t)$.

VI. EXPERIMENT

The samples we used are aqueous dispersions of colloidal particles of tetrafluoroethylene copolymerized with perfluoromethylvinylether (MFA), prepared and kindly donated to us by Ausimont, Milano, Italy. The latex is obtained by a dispersion polymerization process in the presence of an anionic surfactant [5]. By a careful control of the nucleation steps, the process yields fairly monodisperse spherical particles (standard deviation in volume below 5%) with radius around 100 nm. MFA particles are partially crystalline. Their internal structure is probably a conglomerate of some tens of microcrystallites dispersed in an amorphous matrix [5]. Each crystallite is a folded ribbon of polymer chains packed in a regular crystalline structure. The crystallinity should be about 30%, with a chain folding length of the order of 50 nm. The latex particles bear a negative surface charge, which is due in part to adsorbed surfactant and in part to the end groups of the polymer chains (fluorinated carboxyl ions) generated by the decomposition of the initiator.

The light scattering samples were prepared in the following way. The original latex, having a particle volume fraction $\Phi \approx 0.27$, was purified by dialysis until a stable low conductivity value was reached. A small amount of a commercial nonionic surfactant (Triton X-100, produced by Rohm & Haas) was then added to ensure steric stabilization of the particles by surface adsorption. In order to coarsely match the particle and solvent refractive indices and to screen electrostatic interparticle interactions, a second dialysis procedure was performed within a large reservoir containing urea (index of refraction 1.484) at 18% by weight in water with 100 mM NaCl added. Index matching was then further improved by adding urea or water in small amounts until a minimal total scattering cross section of the suspension was reached. Best matching, using a He-Ne incident laser beam, was obtained for a solvent refractive index $n = 1.362$. In this condition, the ratio I_{VV}/I_{VH} at 90° is slightly less than 2. We left the dialyzed latex to sediment in a vessel for about 6 weeks. The iridescent colloidal crystal phase that formed at the bottom of the container was finally extracted. By a density measurement we found that the average particle volume fraction of the crystal phase was 0.552. All samples were prepared by diluting the concentrated latex at $\Phi = 0.552$ with the clear supernatant extracted from the top of the sedimentation vessel. The volume fraction of all the samples was derived by measuring the intensity of the depolarized scattered light I_{VH} and comparing it with the value of I_{VH} given by the concentrated sample. In fact, I_{VH} is insensitive to interparticle interactions [5] and represents therefore a good probe of the particle concentration in the scattering volume [19]. The absolute calibration of the volume fraction was further checked in the following way. From previous studies performed on quite similar latexes at 100 mM ionic strength, we know that the phase diagram closely conforms to the equation of state for a hard-sphere fluid [19]. A concentrated sample was left to equilibrate under gravity in a cell and the depolarized scattering intensity was measured just over and below the meniscus separating the fluid from the colloidal crystal phase. By using the original calibration of the parent sample we get particle volume fractions $\Phi_F = 0.496$ and $\Phi_C = 0.534$ for the coexisting fluid and crystal phases, which is within 3% of the expected values

for a hard-sphere fluid.

Table I gives the sample denominations together with the corresponding particle volume fractions. Samples 15F and 15C refer to a single preparation at $\Phi = 0.517$ that was allowed to phase separate in the scattering cell: by vertically translating the cell, measurements were taken respectively just over (15F) and below (15C) the meniscus separating the fluid and crystal phases in equilibrium. We must, however, put a note of caution about the concentration given for sample 15F: in previous sedimentation experiments on similar particles [19] we have indeed noticed that the time for full equilibration of the fluid layer just over the top of the colloidal crystal is generally much longer than the few hours we waited in the present experiment, so that concentration supersaturation or depletion phenomena cannot be excluded. Accordingly, the results for sample 15F are presented only for completeness and will not be used in the fits of the experimental data. The same experiment conversely did not show similar slow equilibration phenomena in the top layer of the crystallized suspension. We also determined the turbidity of the samples, which is found to increase almost linearly with Φ. This confirms that the scattering at index matching is essentially incoherent. The turbidity attains for $\Phi = 0.55$ the value 0.39 cm^{-1}.

The light scattering apparatus includes a He-Ne laser operating at $\lambda = 632.8$ nm, a cylindrical scattering cell having an optical path of 8 mm immersed in a thermostatted index-matching vat, a photomultiplier tube mounted on a rotating arm, and a multiple-tau digital correlator (Brookhaven Instruments, BI 9000). The vertical polarization of the incident laser beam is improved by a Glan-Thompson prism (Bernard Halle, Berlin) and a second prism in the detection optics permits us to select the observed polarization. The extinction ratio of the crossed polarizers is reduced by the stress birefringence of the cell and vat windows to about 10^{-4}. The scattered intensities I_{VV} and I_{VH} are measured in the horizontal scattering plane. Particular care was taken in reducing the collection of light scattered outside the scattering plane by limiting the vertical width of the collection optics with a narrow aperture. This makes very small the possible depolarization effects due to multiple scattering, thanks to the fact that the light doubly scattered in the scattering plane preserves the incident polarization. Indeed, with the above collection geometry, the I_{VV}/I_{VH} ratio for the light scattered by a suspension of isotropic polystyrene particles of radius $a = 100$ nm having turbidity approximately equal to 0.7 cm^{-1} is still as low as 4×10^{-3}. All measurements were taken at 25 °C with a thermal stability of 0.01 °C . The depolarized intensity correlation function was measured for each sample at seven angles ranging from 15 ° to 135 °.The rotational contribution, yielding a finite correlation time even at vanishing scattering wave vector, has the practical effect of reducing the range of variation of the decay rate of the correlation function [6]. We could then use for all scattering angles (and for all samples) the same set of sampling times, ranging from 0.5 ms to 30 ms in 155 logarithmically spaced channels. The decay rates were determined by using a standard cumulant fit program. Further elaboration and fit to the data were performed using a Levenberg-Marquardt nonlinear fit routine. To give more information about the polydispersity of the used particles, we present in Fig. 1 a depolarized field correlation function measured on the most dilute sample (sample 1) at $\theta = 15°$. The full curve is a best fit with a single exponential with a decay time of 1.42 ms (corresponding to a particle radius of about 110 nm), showing that the degree of polidispersity is indeed very low. Noting that the ratio of the translational to the rotational contribution, given by $D_0^t k^2/(6D_0^r) = (2/9)a^2k^2$, is about 3% at 15° for 110-nm particles, we conclude that the observed decay rate is due only to rotational diffusion and therefore scales as the inverse of the cube of the particle radius. This means that deviations from expo-

TABLE I. Values of the volume fraction, of the translational self-diffusion coefficient, and of the rotational diffusion coefficient for the samples used.

Sample	Φ	$D_t^S(10^{-8}$ cm^2 s$^{-1})$	D_r^S (s^{-1})
1	0.031	1.91±0.09	120.0±2.7
2	0.064	1.80±0.07	117.5±2.3
3	0.098	1.69±0.06	115.0±2.0
4	0.118	1.63±0.05	113.7±1.4
5	0.155	1.47±0.06	111.2±1.8
6	0.189	1.29±0.05	106.9±1.5
7	0.217	1.22±0.05	103.2±1.6
8	0.255	1.09±0.04	97.3±1.4
9	0.287	0.95±0.04	92.3±1.4
10	0.326	0.85±0.05	86.4±1.2
11	0.357	0.74±0.05	80.9±1.2
12	0.394	0.66±0.06	74.0±1.6
13	0.421	0.57±0.05	70.0±1.2
14	0.453	0.50±0.06	65.5±1.4
15F	0.485	0.45±0.09	61.6±2.2
15C	0.534	0.38±0.05	58.1±1.4

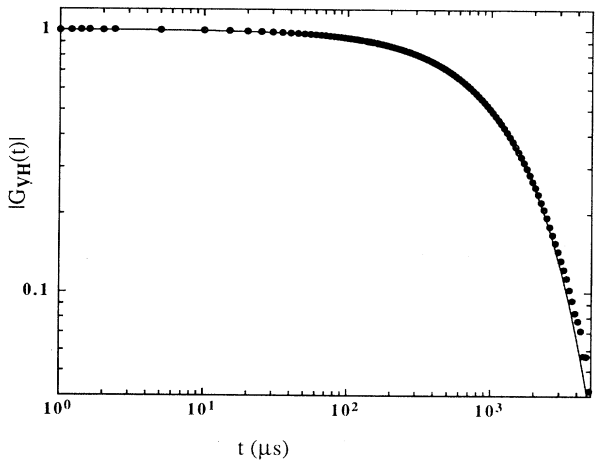

FIG. 1. Correlation function $|G_{VH}(t)|$ of the depolarized scattered field measured at the scattering angle $\theta = 15°$. The full line is a fit with an exponential having a time constant of 1.42 ms.

nentiality are related to polydispersity of the particle volume. A two cumulant fit gives a volume polydispersity of about 5%, which corresponds to a radius polydispersity less than 2%, a figure that is lower than the best values for polystyrene particles used as calibration standards.

VII. ANALYSIS OF THE EXPERIMENTAL DATA

A. Short-time translational and rotational self-diffusion

Figure 2 shows the first cumulant of the VH correlation function versus the squared modulus of the $\boldsymbol{k}$ vector for three of the samples we used, showing the predicted linear dependence on k^2 with nonzero intercept. Linear fits to the whole set of Γ versus k^2 plots yield the concentration dependence of the translational and rotational self-diffusion coefficients, which are shown in Figs. 3 and 4. The fit was limited to measurements performed in the fluid phase with exclusion of sample 15F. Error bars correspond to one standard deviation determined using as input the standard deviations of the fits to each Γ vs k^2 plot. To increase the accuracy of the intercept, measurements at the lowest k were taken by using a much longer accumulation time (typically 20 min). Notice that the relative accuracy of D_r^S is better for large volume fractions, where the fractional contribution of translational diffusion is smaller. From the low-concentration limit for D_t^S and D_r^S we can derive a more precise value for the particle size [6]: indeed the particle radius can be obtained from $a = (3D_0^t/4D_0^r)^{1/2} = (110 \pm 2)$ nm. Such an expression has the advantage of being independent of the solvent viscosity and temperature.

As can be seen from Figs. 3 and 4, both the rotational and the translational self-diffusion coefficients monotonically decrease as the particle volume fraction is increased. The translational self-diffusion data are compared in Fig. 3 with the theoretical predictions for hard spheres. The full line has been drawn by fixing the first

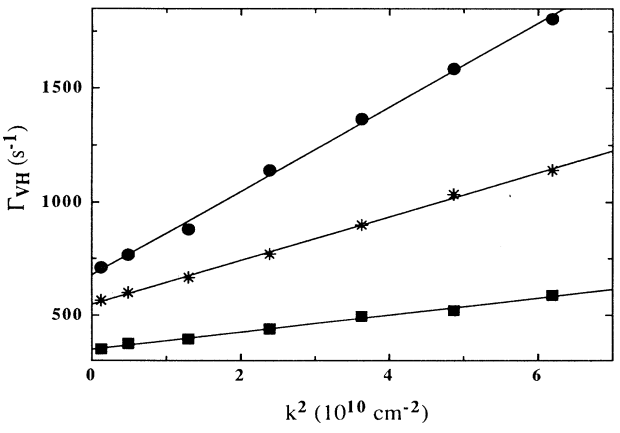

FIG. 2. First cumulant of $|G_{VH}(t)|$ plotted versus the square modulus of the scattering vector for three distinct samples: dots refer to sample 4, stars to sample 9, squares to sample 15C.

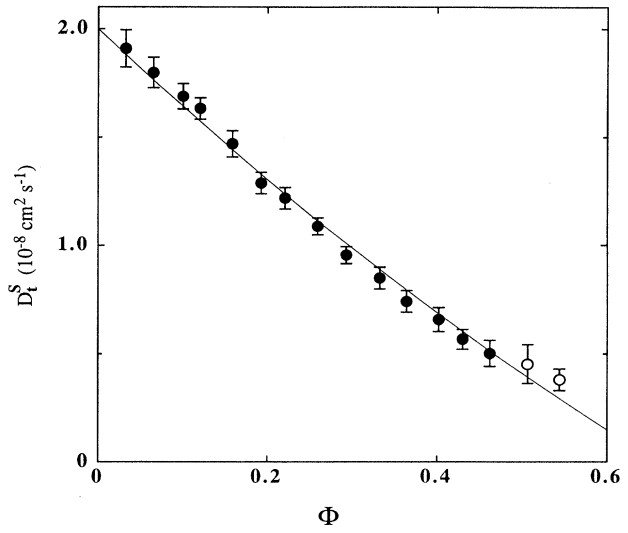

FIG. 3. Short-time translational self-diffusion coefficient D_t^S plotted as a function of the volume fraction Φ. The full line represents a polynomial fit including linear and quadratic terms. The two points at the largest volume fractions (open dots), which refer to samples 15F and 15C, are excluded from the fit.

virial coefficient to the accurate value calculated by Cichocki and Felderhof [13] and fitting a Φ^2 term to the data. The result of the best fit is

$$D_t^S = (2 \pm 0.02) \times 10^8[1 - 1.83\Phi + (0.5 \pm 0.1)\Phi^2] \text{ cm}^2/\text{s}. \quad (57)$$

The value of the coefficient H_{s2}^t is slightly lower than

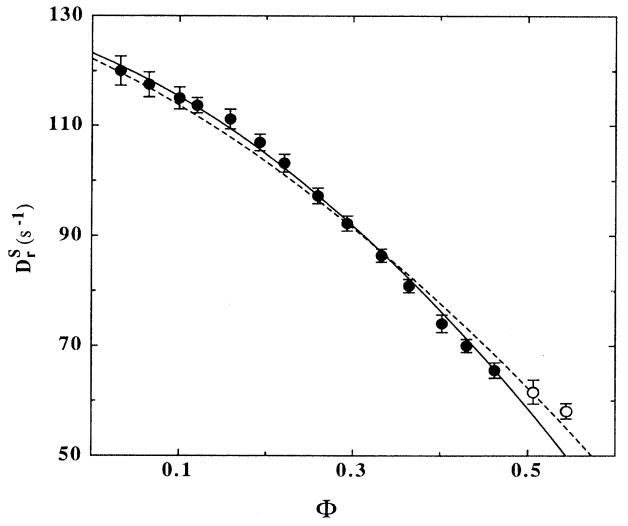

FIG. 4. Short-time rotational diffusion coefficient D_r^S plotted as a function of the volume fraction Φ. The full line represents a polynomial fit including linear and quadratic terms. The two points at the largest volume fractions (open dots), which refer to samples 15F and 15C, are excluded from the fit. The dotted line is the theoretical prediction calculated in Sec. IV.

the theoretical value calculated by Beenakker and Mazur [14]. Note that these authors obtained also a smaller value for H_{s1}^t ($H_{s1}^t = -1.73$) because of the limited number of terms included in their expansion. Our experimental results agree within error bars with previous measurements by van Veluwen *et al.* [20] and by van Megen and Underwood [21] performed with different techniques. We also find good agreement with the numerical simulation results [22].

An interesting question is the effect of the crystal phase on the short-time self-diffusion coefficient. Our data suggest a slight relative increase of D_t^S compared to the value expected by extrapolation of the fluid-phase data. This suggests that the tracer mobility in the dense fluid is slightly less than in the crystal at essentially the same volume fraction. We can understand this qualitatively by observing that crystallization in a hard-sphere suspension implies a substantial increase of the configurational entropy associated with the extra free volume per particle available in the crystal as opposed to the fluid phase. Since the hydrodynamic interaction effect on a tracer should be less if there is more free volume (greater mean interparticle separation) we might expect D_t^S to be slightly enhanced in the crystal phase. The fact that the trend of the translational self-diffusion coefficient closely conforms to the existing theoretical predictions and experimental data strongly supports the validity of the decoupling approximation at short times for all volume fractions.

Figure 4 shows the results for the short-time rotational self-diffusion coefficient. First of all, D_r^S presents a behavior markedly different from that found for D_t^S: indeed, the slope of the D_r^S versus Φ curve becomes steadily more negative with increasing Φ. This clearly means that (a) the coefficient H_{s2}^r in the virial expansion has to be negative and (b) its magnitude relative to H_{s1}^r is much larger than in the case of translational diffusion, where a very limited deviation from linearity in Φ is observed over the whole concentration range. The dotted line in Fig. 4 is the theoretical prediction given in Eq. (40). The agreement is rather good, although the experimental data seem to show a slightly smaller initial slope and conversely a slightly larger downward curvature. Indeed, a best fit to a second degree polynomial with all parameters free (full line) gives

$$D_r^S = (123.3 \pm 1.5) \times [1 - (0.55 \pm 0.08)\Phi - (1.1 \pm 0.2)\Phi^2]\,\mathrm{s}^{-1}. \quad (58)$$

It is possible that the agreement between experiment and theory could improve by adding higher-order terms in the virial expansion. It should also be taken into account that the value of H_{s1}^r is extremely sensitive to the pair correlation function near touching [3,8,23], due to the overwhelming importance for rotational diffusion of very short-distance hydrodynamic contributions. It is therefore possible that the ionic strength of the used colloidal suspensions is not large enough to completely screen Coulomb repulsions. It is known that the effect of residual electrostatic interactions that prevent particles from coming into close contact is that of reducing H_{s1}^r, whereas no prediction is available about the influence on the higher-order terms.

B. Long-time behavior

In this section we discuss the full shape of the rotational correlation function. We assume, first of all, that the correlation function measured at the smallest accessible scattering angle $\theta_{\min}$ is purely rotational. Indeed, we note that for the scattering wave vector $k_{\min} = 1.24 \times 10^{-9}\ \mathrm{cm^2\,s^{-1}}$ corresponding to $\theta_{\min}$, the translational contribution to the initial decay of the correlation function ranges from 3.3% for sample 1 down to 1.4% for sample 15C. Within the decoupling approximation this suggests that the correlation functions measured at $k_{\min}$ are purely rotational to a good degree of approximation. We call $G_{VH}(t,\Phi)$ the correlation function taken at $k_{\min}$ with the sample at volume fraction Φ and we call Φ_1 the lowest used volume fraction (sample 1). We can then write

$$\frac{G_{VH}(t,\Phi)}{G_{VH}(t,\Phi_1)} = \frac{1+\Phi\gamma_2(t)}{1+\Phi_1\gamma_2(t)} = 1 + (\Phi - \Phi_1)\gamma_2(t) \quad (59)$$

so that $\gamma_2(t)$ can be calculated as

$$\gamma_2(t) = \frac{G_{VH}(t,\Phi)/G_{VH}(t,\Phi_1) - 1}{\Phi - \Phi_1}. \quad (60)$$

Figure 5 shows the experimental $\gamma_2(t)$ for some of the measured samples. We find that all the data relative to $\Phi \leq 0.2$ fall approximately on the same curve, which closely follows the theoretical prediction [8]. Figure 5 shows that, for $\Phi > 0.2$, the experimental curves start with a larger initial slope and acquire a larger and larger upward curvature. It is simple to account for the increase

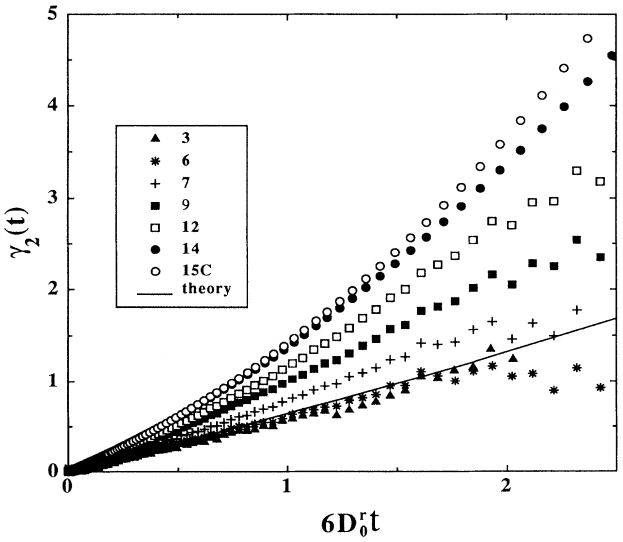

FIG. 5. Measured function $\gamma_2(t)$ plotted as a function of normalized time $6D_0^r t$ for seven distinct volume fractions (listed in the inset). The full line represents the theoretical prediction for low volume fractions.

of the initial slope if we note that, including the Φ^2 term in the virial expansion for D_r^S, the short-time expression for $\gamma_2(t)$ should be

$$\gamma_2(t) = -6D_0^r t\,[H_{s1}^r + H_{s2}^r(\Phi + \Phi_0)]. \tag{61}$$

Figure 6 shows the experimentally determined quantity

$$s_\gamma = \frac{1}{6D_0^r} \lim_{t\to 0} \frac{d\gamma_2}{dt} \tag{62}$$

as a function of Φ. The full line represents the behavior predicted by Eq. (61), using the best fit values for H_{s1}^r and H_{s2}^r. We see that the agreement is good.

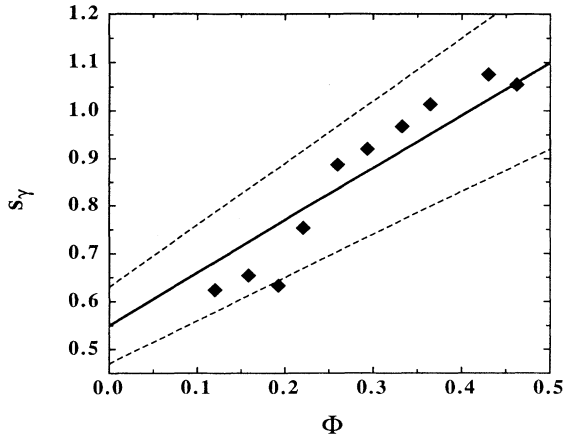

FIG. 6. Initial slope of $\gamma_2(t)$ plotted as a function of the volume fraction. The full line represents the prediction, as calculated from Eq. (61). The dashed lines represent lower and upper bounds for the predicted values, once the experimental uncertainty in the evaluation of the parameters is taken into account.

VIII. CONCLUSIONS

In this article we have presented experimental and theoretical results concerning orientational relaxation and translational self-diffusion in hard-sphere colloidal suspensions. By using index-matched suspensions of intrinsically anisotropic spheres, we have performed depolarized dynamic light scattering measurements in a wide range of volume fractions up to the colloidal-crystal region. We have obtained the Φ dependence of the short-time rotational diffusion coefficient and of the short-time translational self-diffusion coefficient. In the case of D_t^S we have good agreement with previous theoretical and experimental results. Concerning D_r^S, we have presented theoretical calculations that give the value of the coefficient of the Φ^2 term by taking into account lowest-order three-body hydrodynamic effects. We find that the predicted behavior of D_r^S is in good agreement with the experimental results. Our data show that the coefficient of the Φ^2 term has the same (negative) sign presented by the linear term. Such behavior is different from that found for translational self-diffusion. We have also measured the full shape of the orientational correlation function $F_r(t)$, which shows an increasing deviation from exponential behavior as Φ grows. For $\Phi < 0.2$ such a deviation shows an interesting scaling property, in agreement with the theoretical predictions.

ACKNOWLEDGMENTS

This work was partially supported by funds from the Italian Ministry for University and Research (MURST).

[1] R. B. Jones and P. N. Pusey, Annu. Rev. Phys. Chem. **42**, 137 (1991).
[2] P. N. Pusey, in *Liquids, Freezing and Glass Transition*, edited by J. P. Hansen, D. Levesque, and J. Zinn-Justin (North-Holland, Amsterdam, 1991).
[3] R. B. Jones, Physica A **150**, 339 (1988).
[4] R. Piazza, J. Stavans, T. Bellini, D. Lenti, M. Visca, and V. Degiorgio, Prog. Colloid Polym. Sci. **91**, 89 (1990).
[5] V. Degiorgio, R. Piazza, T. Bellini, and M. Visca, Adv. Colloid Interface Sci. **48**, 61 (1994).
[6] R. Piazza, V. Degiorgio, M. Corti, and J. Stavans, Phys. Rev. B **42**, 4885 (1992).
[7] B. J. Berne and R. Pecora, *Dynamic Light Scattering* (Wiley, New York, 1976).
[8] R. B. Jones, Physica A **157**, 752 (1989).
[9] R. Schmitz and B. U. Felderhof, Physica A **116**, 163 (1982).
[10] B. Cichocki, B. U. Felderhof, and R. Schmitz, Physicochem. Hyd. **10**, 383 (1988).
[11] R. B. Jones and R. Schmitz, Physica A **149**, 373 (1988).
[12] G. K. Batchelor, J. Fluid Mech. **74**,1 (1976).
[13] B. Cichocki and B. U. Felderhof, J. Chem. Phys. **89**, 1049 (1988).
[14] C. W. J. Beenakker and P. Mazur, Physica A **120**, 388 (1983).
[15] B. U. Felderhof, G. W. Ford, and E. G. D. Cohen, J. Stat. Phys. **28**, 135 (1982).
[16] J. G. Kirkwood, J. Chem. Phys. **3**, 300 (1935).
[17] P. Mazur and W. van Saarloos, Physica A **115**, 21 (1982).
[18] P. Reuland, B. U. Felderhof, and R. B. Jones, Physica A **93**, 465 (1978).
[19] R. Piazza T. Bellini, and V. Degiorgio, Phys. Rev. Lett. **71**, 4267 (1993).
[20] A. van Veluwen, H. N. W. Lekkerkerker, C. G. de Kruyf, and A. Vrij, J. Chem. Phys. **89**, 2810 (1988).
[21] W. van Megen and S. M. Underwood, J. Chem. Phys. **91**, 552 (1989).
[22] A. J. C. Ladd, J. Chem. Phys. **93**, 3484 (1990).
[23] R. Piazza, and V. Degiorgio, J. Phys. Condens. Matter. **5**, B173 (1993).